

SCIENCES

*Waves, Field Directors – Pierre-Noël Favennec, Frédérique de Fornel*

---

*Electromagnetism, Subject Head – Pierre-Noël Favennec*

# **Electromagnetic Waves 1**

*Maxwell's Equations, Wave Propagation*

*Coordinated by*  
**Pierre-Noël Favennec**

Color Section

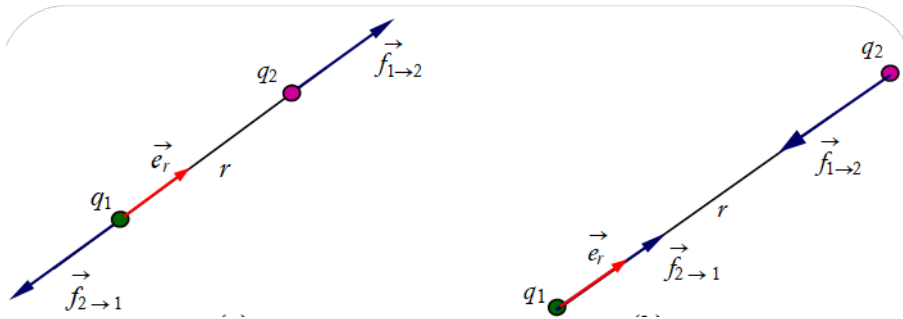


**Figure 1.1.** Coulomb forces between two point and fixed charges  $q_1$  and  $q_2$

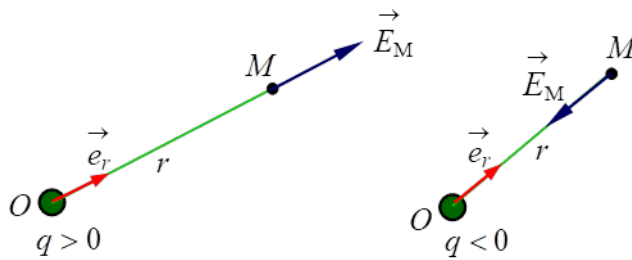


**Figure 1.2.** Electrostatic field  $\vec{E}_M$  created by a fixed point charge  $q$

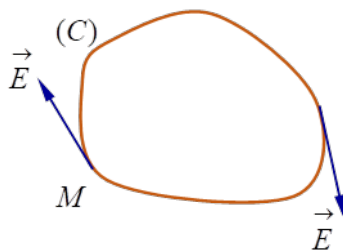


**Figure 1.3.** Circulation of the electrostatic field about a closed contour  $(C)$

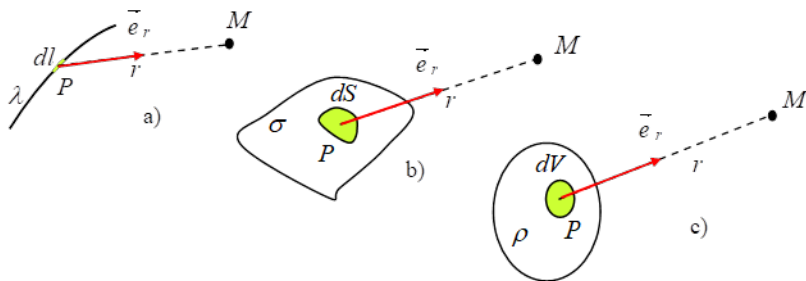


**Figure 1.4.** Continuous charge distributions

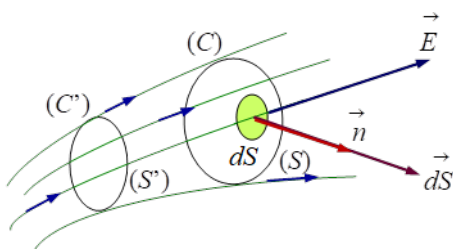


**Figure 1.5.** Electrostatic field lines

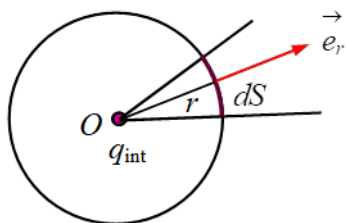


**Figure 1.6.** Charge  $q_{int}$  at the center O of a sphere with radius  $r$

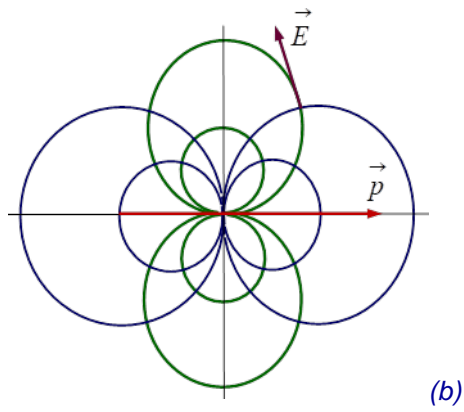
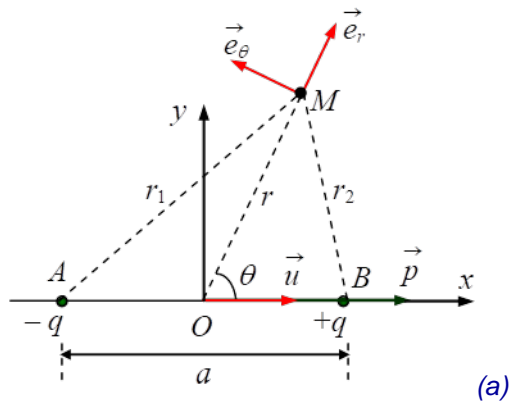


**Figure 1.7.** a) Electrostatic dipole; b) field lines (in green) and equipotential surfaces (in blue) of an electrostatic dipole

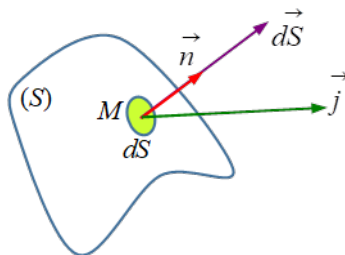


**Figure 1.8.** Current density vector at point M

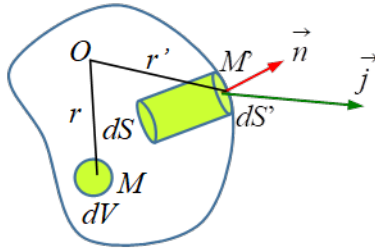


**Figure 1.9.** Current density vector at point  $M'$

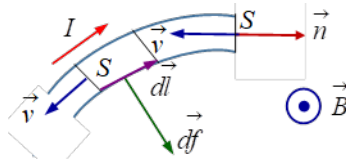


**Figure 1.10.** Portion of a conductor with section  $s$ , traversed by a current with intensity  $I$

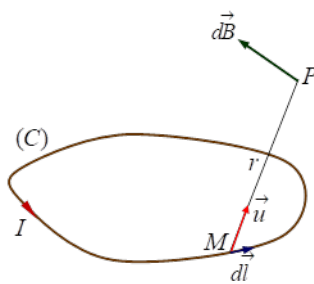


**Figure 1.11.** Magnetic field  $d\vec{B}$  created by an element with a length  $dl$  of a circuit  $(C)$

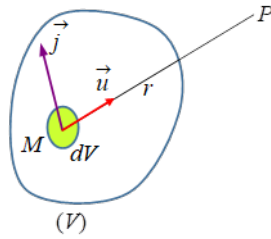


**Figure 1.12.** Current distribution within volume  $V$

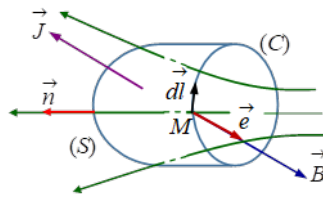


**Figure 1.13.** Circulation of a magnetic field on a contour  $(C)$

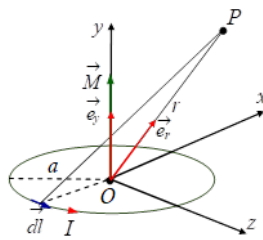


**Figure 1.14.** Magnetic dipole composed of a circular coil with magnetic moment  $M$

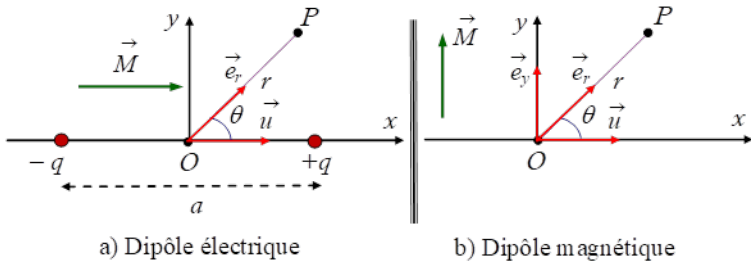


**Figure 1.15.** Analogy a) electric dipole; b) magnetic dipole

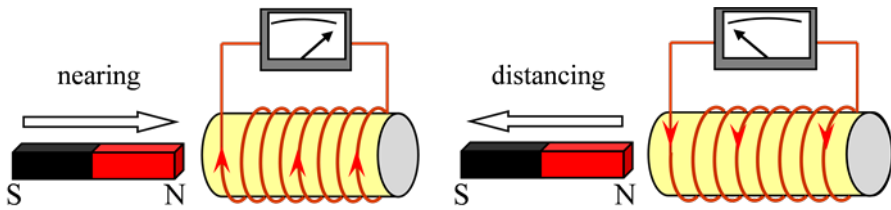


**Figure 1.16.** a) Magnet far from the coil axis: an electric current occurs; b) magnet close to the axis of the current: an electric current occurs

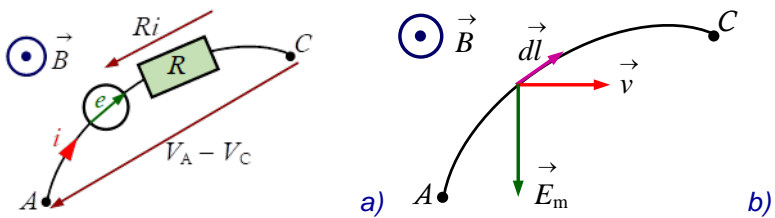


**Figure 1.17.** a) Portion AC of a conductor in motion in a magnetic field; b) electric circuit equivalent to conductor A

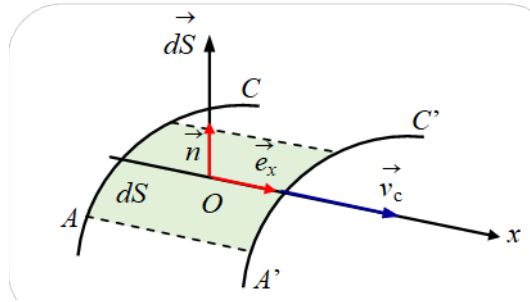


**Figure 1.18.** Area swept by a section AC of the filiform conductor in motion

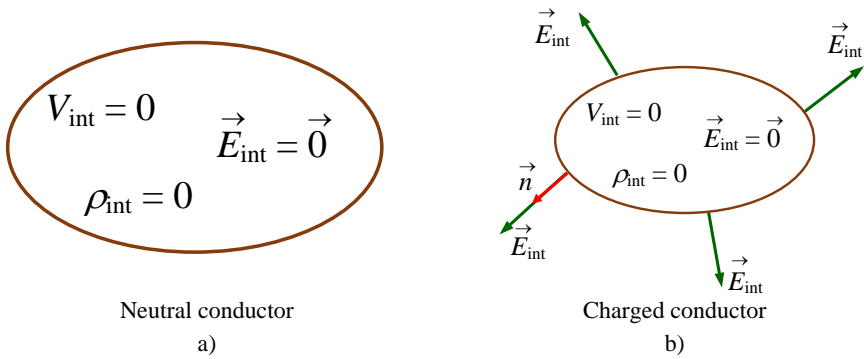


**Figure 1.19.** Conductors in equilibrium

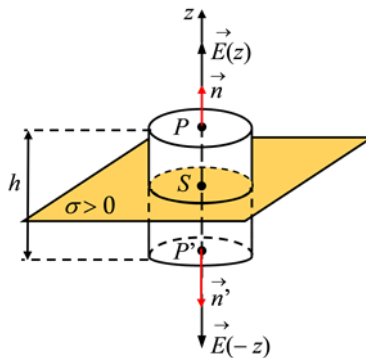


**Figure 1.20.** Electrostatic field surrounding a flat charged surface

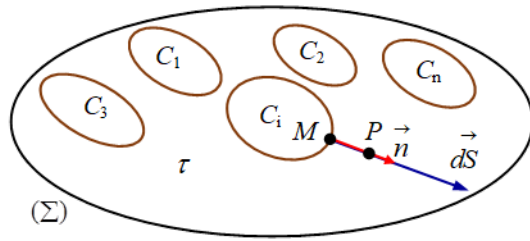


**Figure 1.21.** Conductors in equilibrium

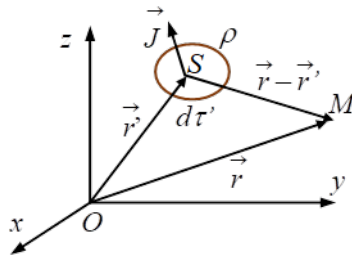


**Figure 1.22.** Sources ( $S$ ) of charges and currents

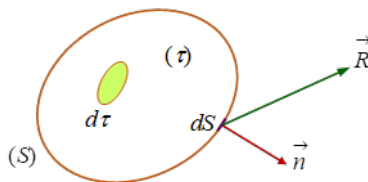


**Figure 1.23.** Surface  $S$  surrounding volume  $V$  containing charge carriers

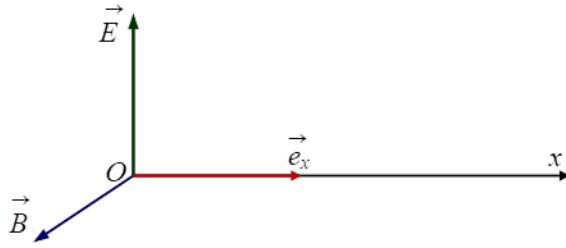


**Figure 1.24.** *Electric and magnetic fields perpendicular and orthogonal to the propagation direction of the progressive plane wave*

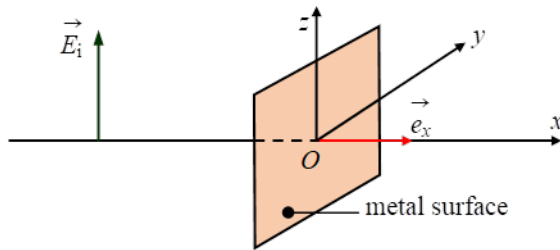


**Figure 1.25.** *Perfect metal arranged vertically on the propagation axis of a monochromatic progressive plane wave*

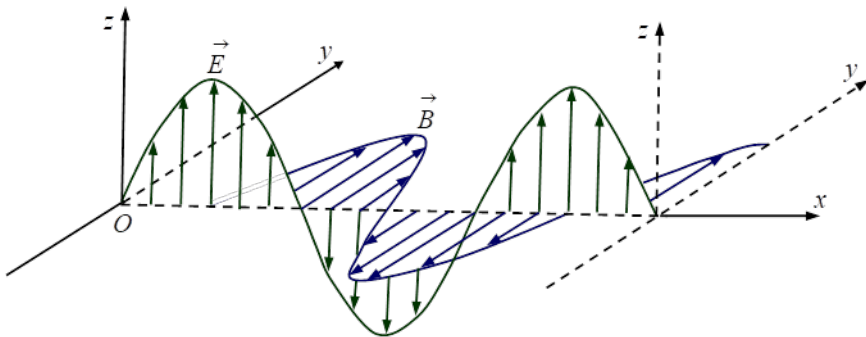


**Figure 1.26.** *Structure of an electromagnetic stationary wave*



**Figure 1.27.** Most likely arrangement of dipole moments of the most stable polar molecules

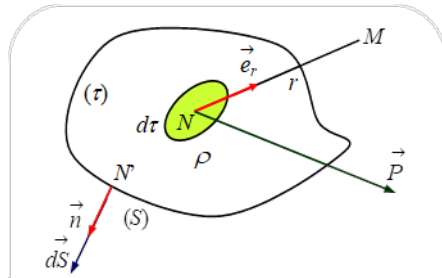


**Figure 1.28.** Dielectric medium with volume  $\tau$

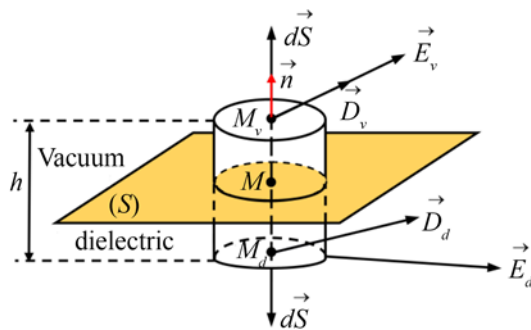


**Figure 1.29.** Refraction of the electric displacement vector across a vacuum-dielectric surface of separation

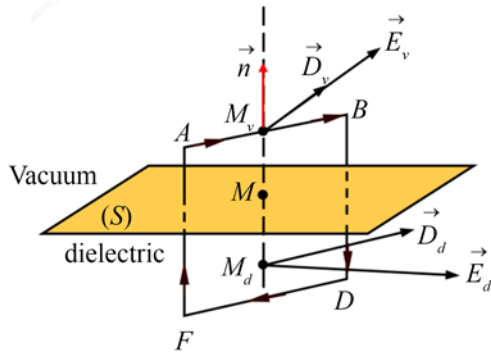


**Figure 1.30.** Circulation of the electric field along an ABDF circuit overlapping a vacuum-dielectric surface of separation

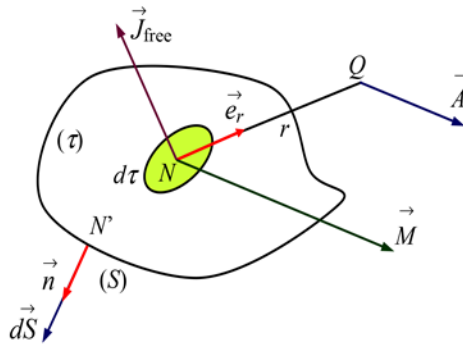


**Figure 1.31.** Magnetic medium with volume  $\tau$

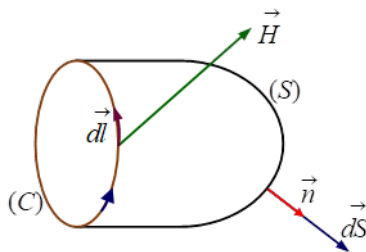


**Figure 1.32.** Circulation of the excitation magnetic vector on a closed contour (C)

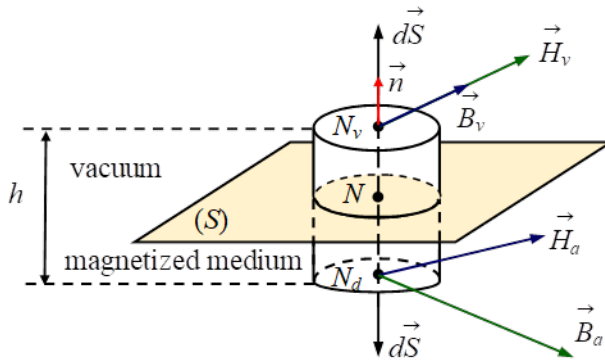


**Figure 1.33.** Refraction of the magnetic field crossing a vacuum-magnetic medium surface of separation

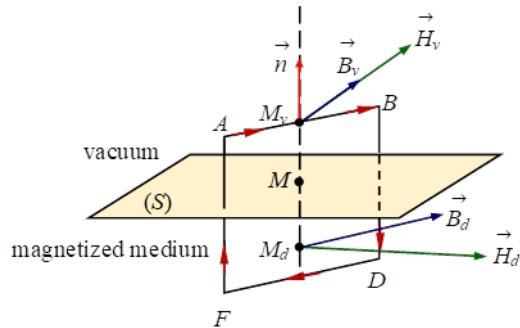


**Figure 1.34.** Circulation of the magnetic field along an ABDF circuit overlapping a vacuum-magnetic medium surface of separation

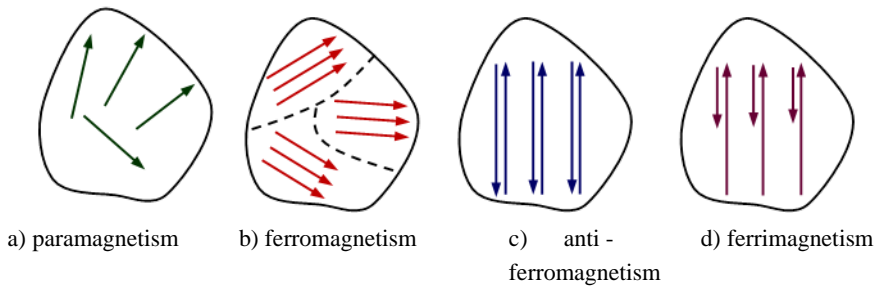


**Figure 1.35.** *Illustration of the different types of magnetism: a) magnetic moments distributed irregularly; b) magnetic moments aligned in a Weiss domain (10  $\mu\text{m}$  to 1 m); c) antiparallel magnetic moments with equal intensities; d) antiparallel magnetic moments with different intensities*

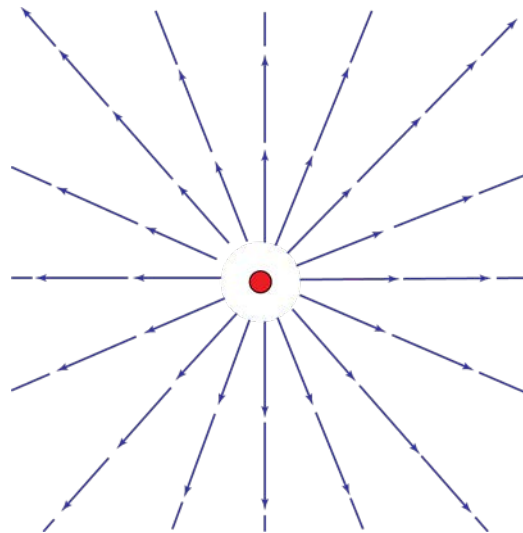


**Figure 2.1.** *Configuration of field lines of the electric field*

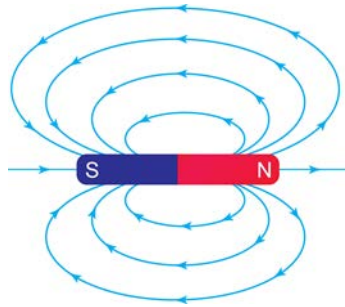


**Figure 2.2.** Configuration of magnetic field lines

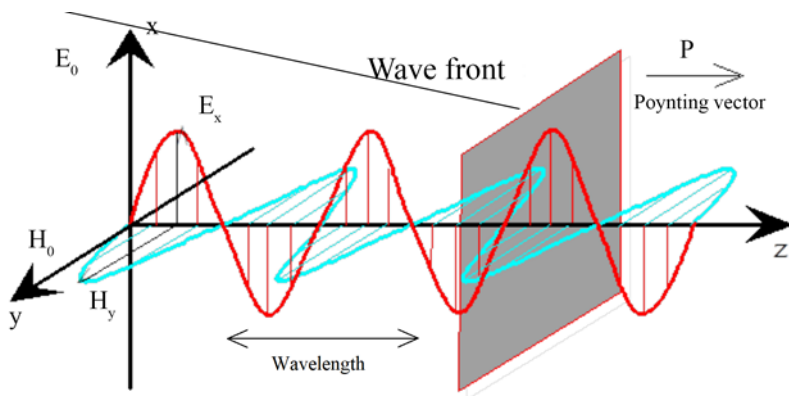


**Figure 2.3.** Diagram depicting the propagation of an electromagnetic wave

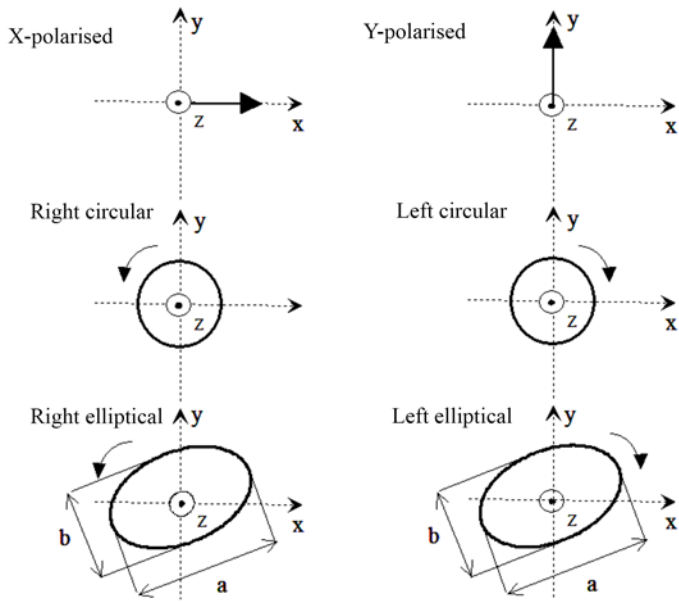


**Figure 2.4.** *The different polarization states for a wave propagating in direction  $z$*

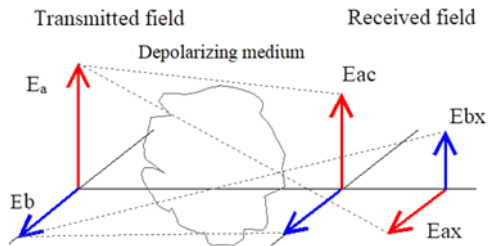


**Figure 2.5.** *Schematic of transpolarization*

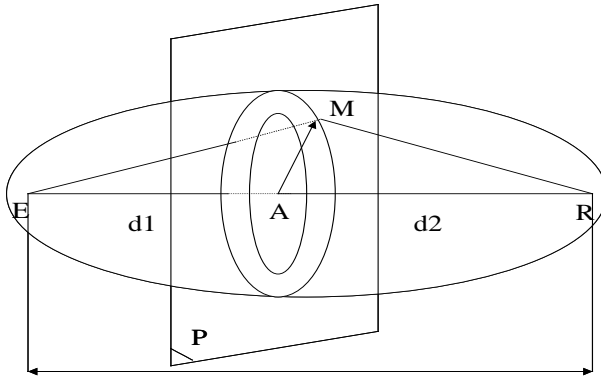


**Figure 2.6.** Schematic representation of Fresnel zones

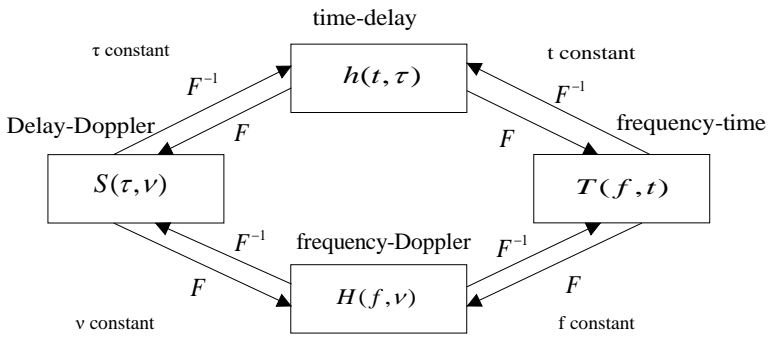


**Figure 2.7.** Representation of the different Fourier transforms on impulse response

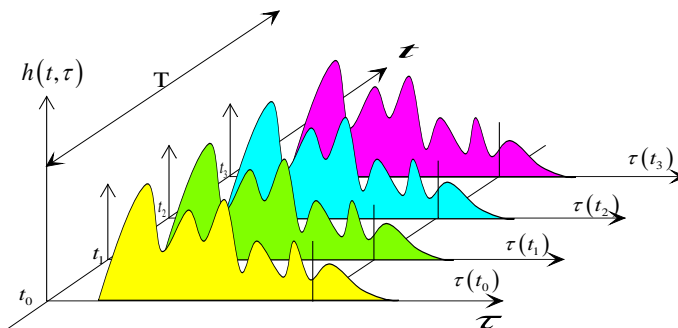


**Figure 2.8.** Representation of the temporal evolution of the propagation channel impulse response

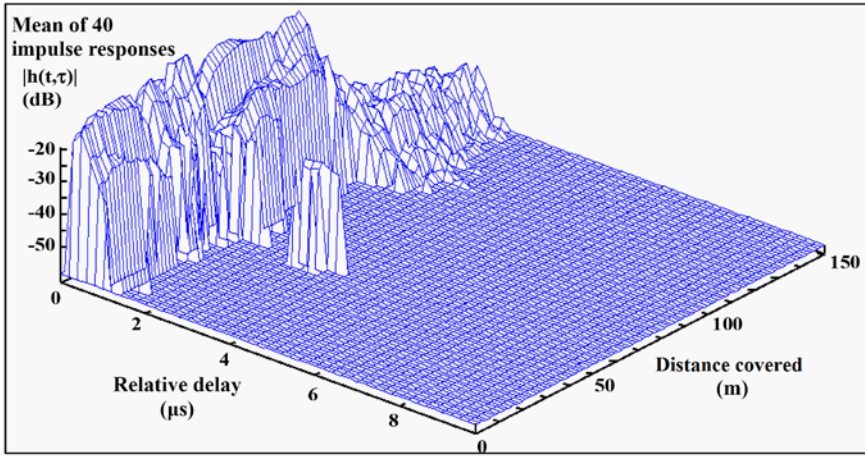


**Figure 2.9.** Evolution of the impulse response: turning a street corner in the microcellular environment (Paris, 900 MHz, FTR&D sounder)

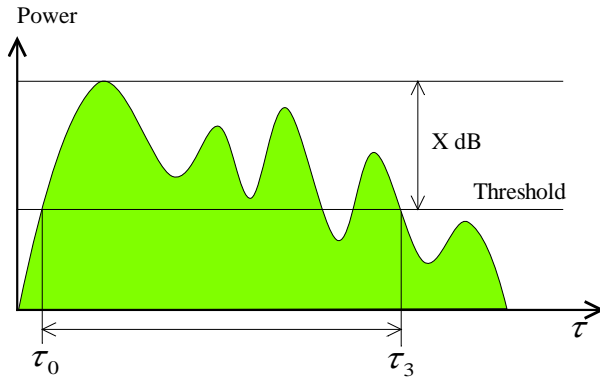


**Figure 2.10.** Example of a power delay profile; highlighted by the delay interval at X dB

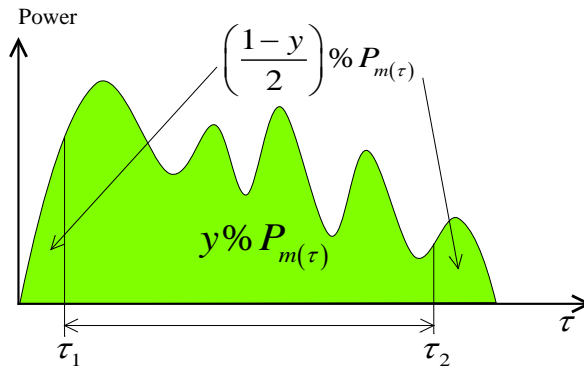


**Figure 2.11.** Example of a power delay profile; highlighted by the delay window at  $y\%$

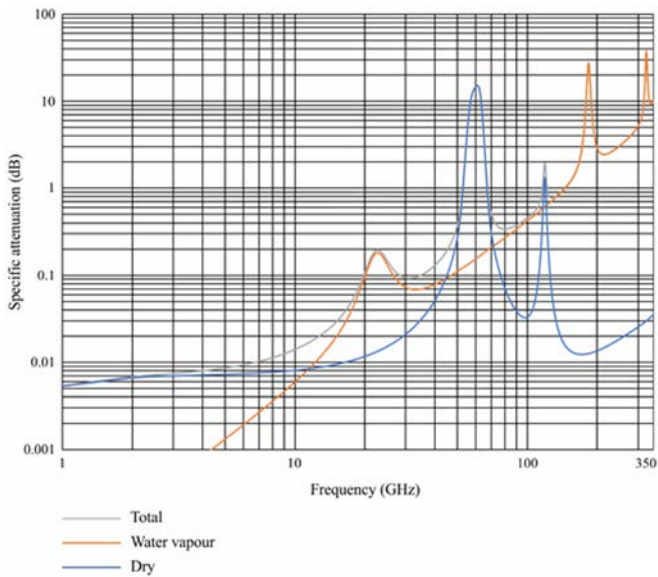


**Figure 2.12.** Specific attenuation (dB/km) due to atmospheric gases ( $O_2$  and  $H_2O$ ) and total (ITU-R P.676)

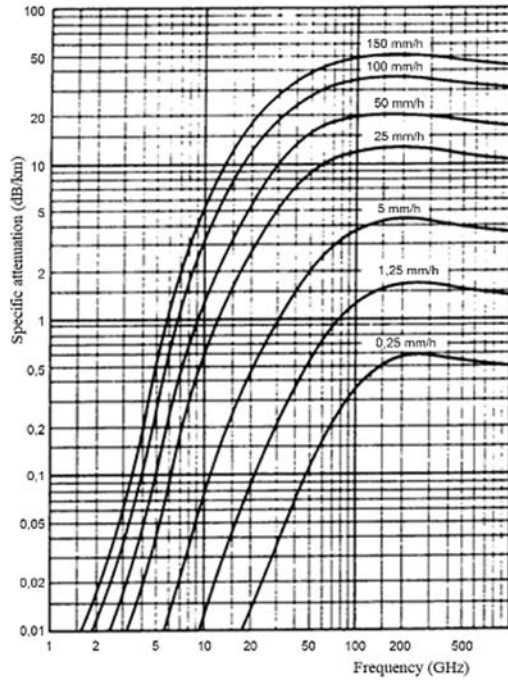


**Figure 2.13.** Specific attenuation (dB/km) due to rain as a function of the frequency (ITU-R P.837)

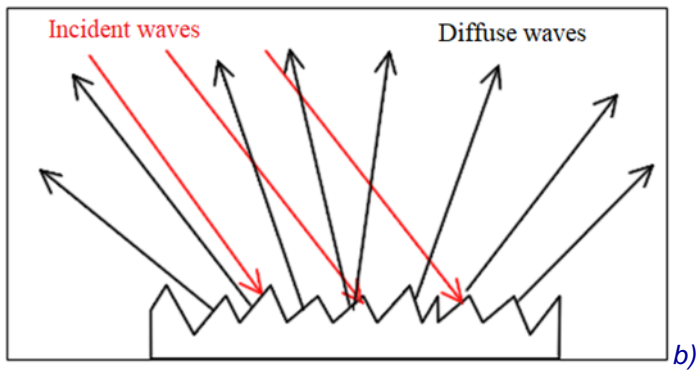
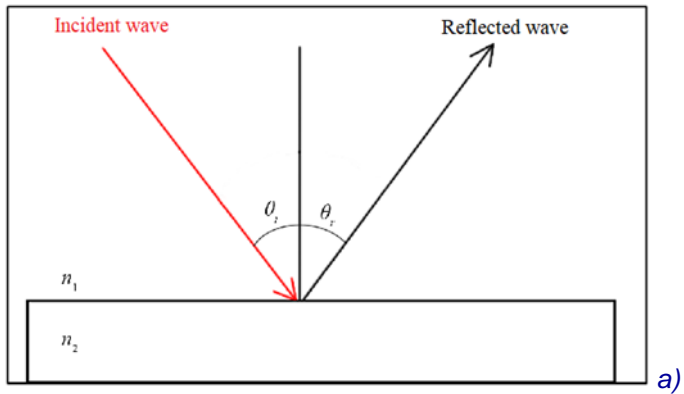


**Figure 2.14.** a) representation of specular reflection;  
b) representation of diffuse reflection

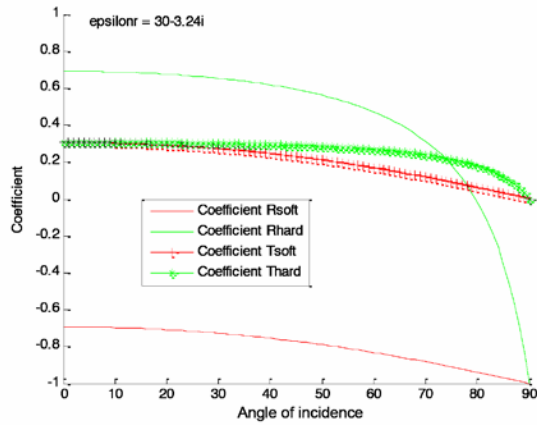


**Figure 2.15a.** Example of the variation of the real part of reflection and transmission coefficients of wet soil at 1 GHz in vertical (hard) and horizontal (soft) polarizations

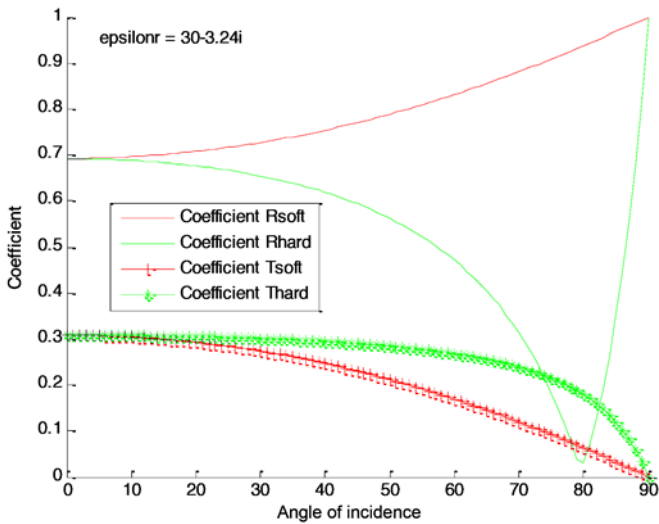


**Figure 2.15b.** Example of the variation of the modulus of the reflection and transmission coefficients of wet soil at 1 GHz in vertical (hard) and horizontal (soft) polarizations

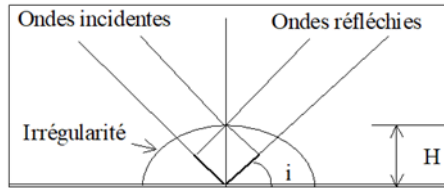


**Figure 2.16.** *Difference in path created by a surface irregularity with height  $H$*

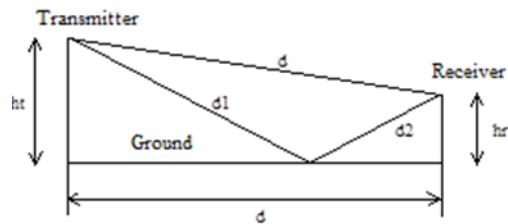


**Figure 2.17.** *Two-line model*

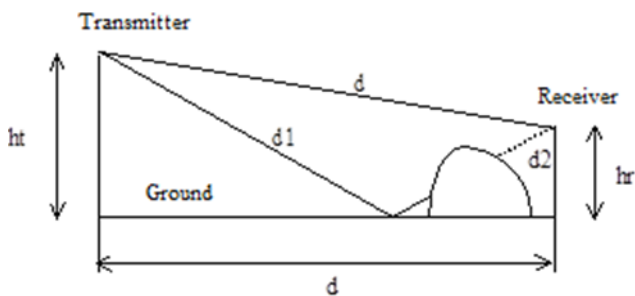


**Figure 2.18.** *Diagram showing the blocking of the reflected ray with an obstacle*

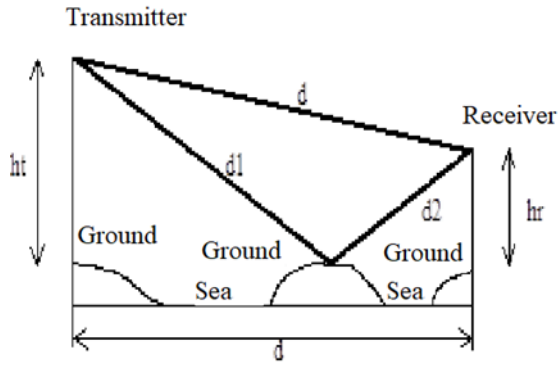


**Figure 2.19.** Diagram showing the path reflected on an island to limit the effect of the reflected path on a maritime link

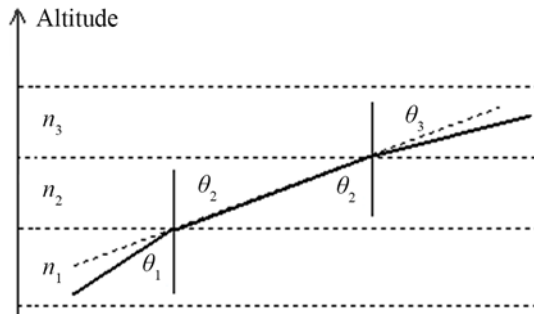


**Figure 2.20.** Geometries associated with Descartes law

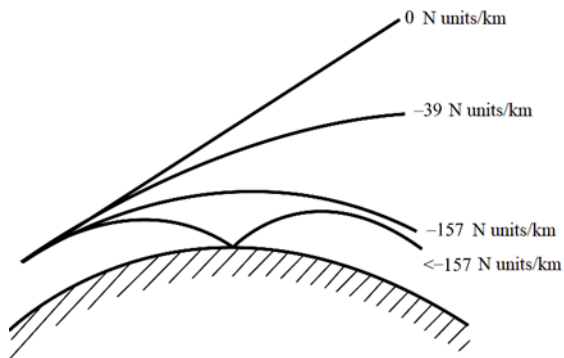


**Figure 2.21.** Paths of radioelectric waves as a function of refractivity gradient

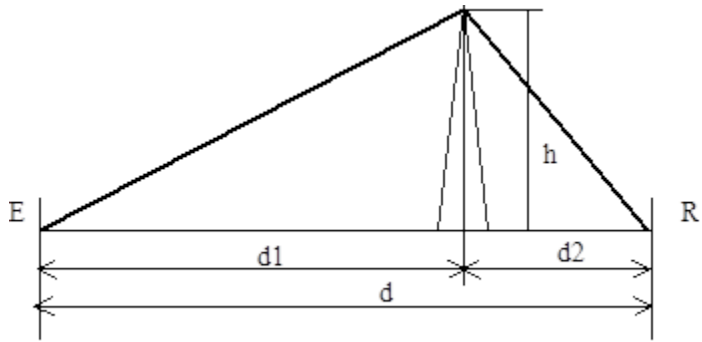


**Figure 2.22.** Representation of a sharp diffracting edge

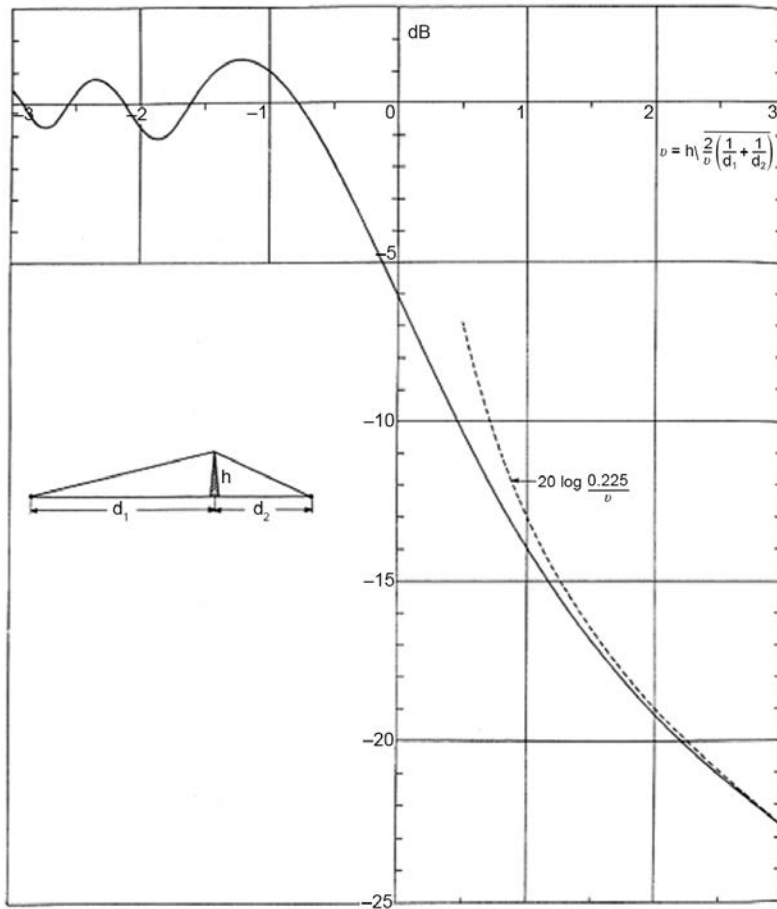


**Figure 2.23.** Attenuation due to diffraction off an edge

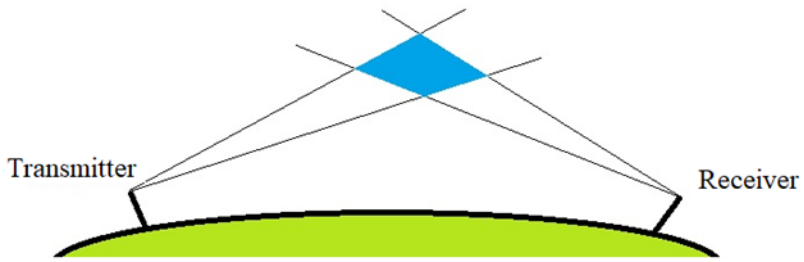


**Figure 2.24.** Propagation of an electromagnetic wave by tropospheric scattering

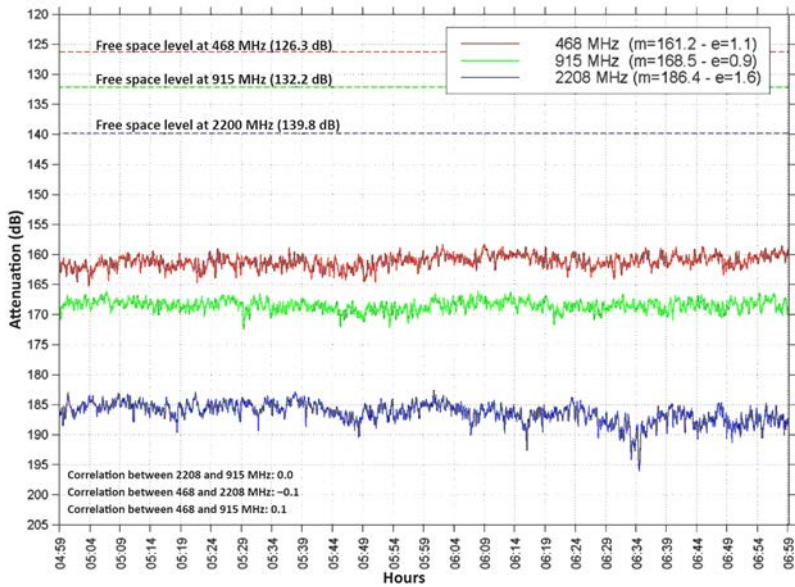


**Figure 2.25.** Example of variation in the radioelectric field due to tropospheric scattering

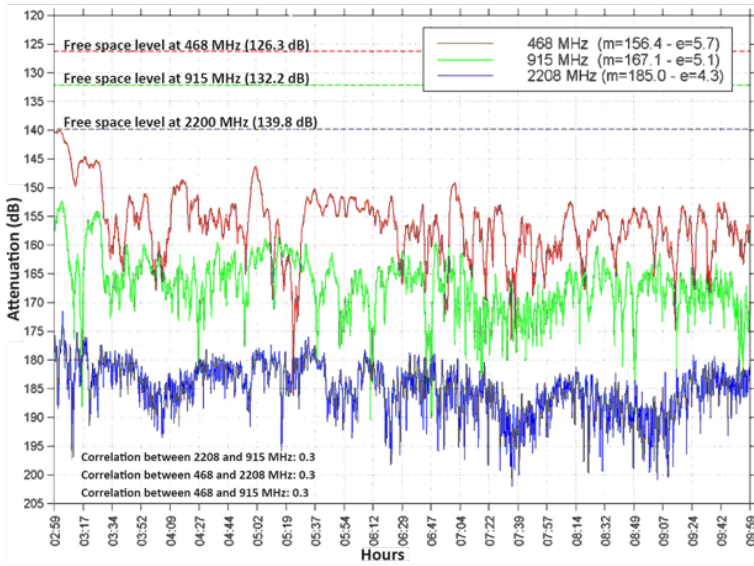


**Figure 2.26.** Example of variation in the radioelectric field due to reflection on layers of the atmosphere

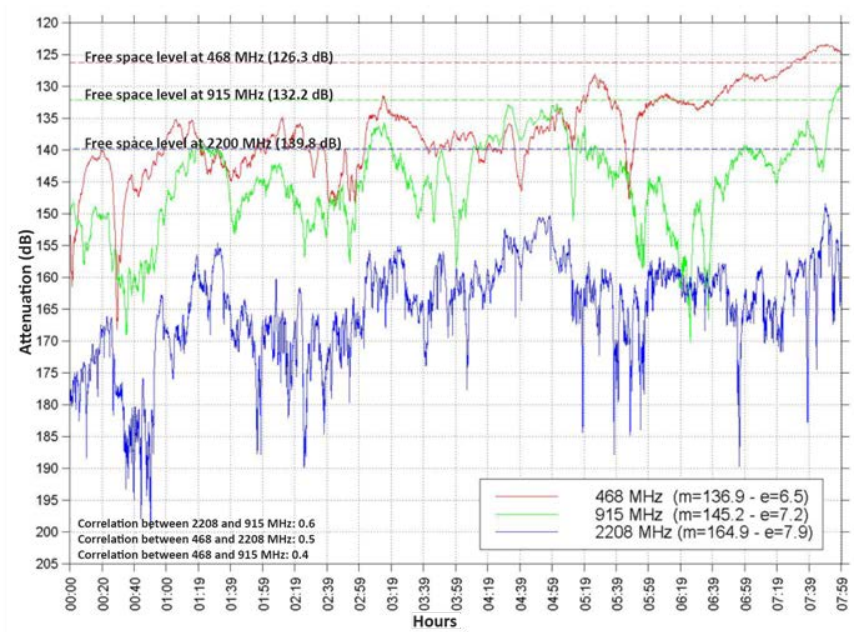


**Figure 2.27.** Example of variation in radioelectric field due to the presence of ducts



**Figure 2.28.** Map of the topography (relief) in the Perpignan region, France

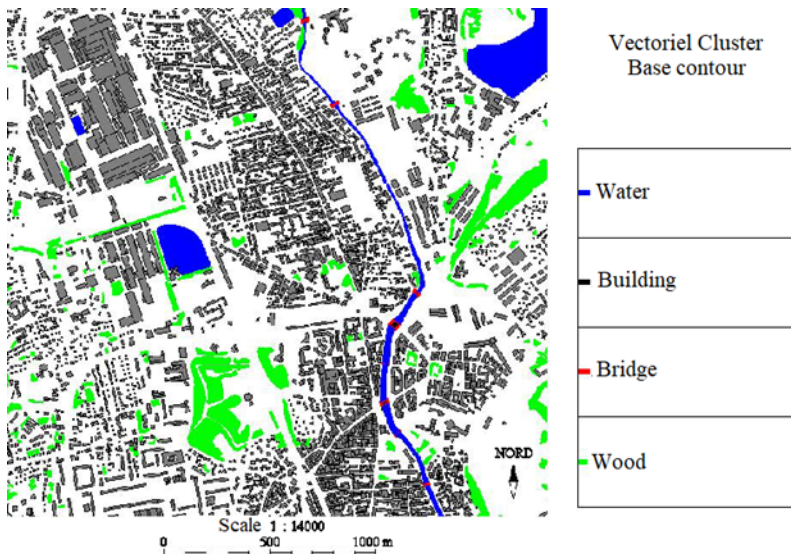


**Figure 2.29.** Map of the topography (relief) in the Belfort region, France

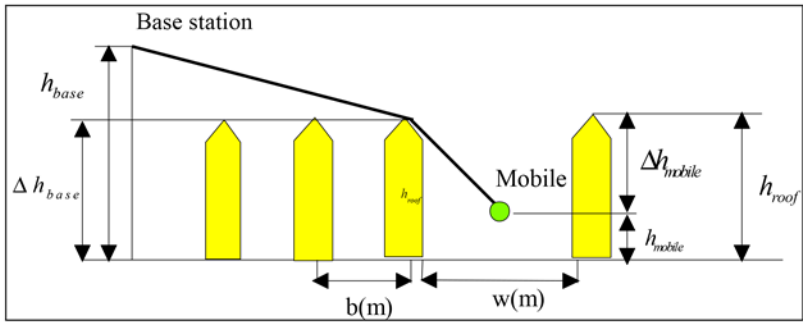


**Figure 2.30.** Schematic representation of the “transmitter-receiver” profile

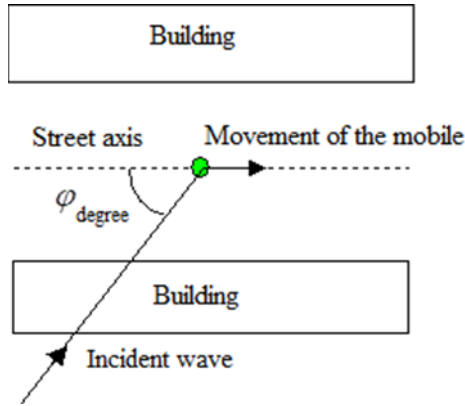


**Figure 2.31.** Definition of the angle between the street axis and the direction of the incidence angle

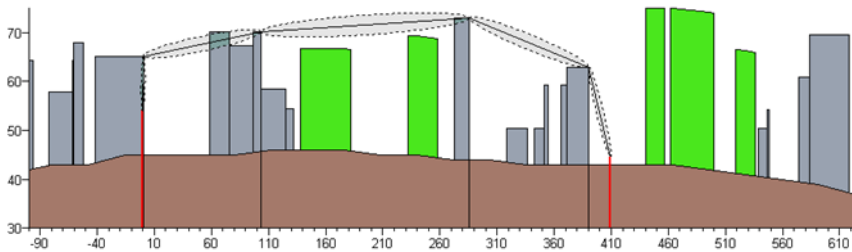


**Figure 2.32.** Example of a “transceiver” profile

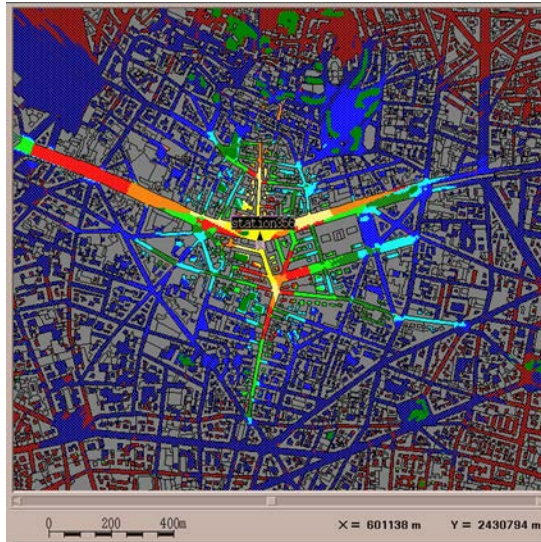


**Figure 2.33.** *Example of urban coverage*

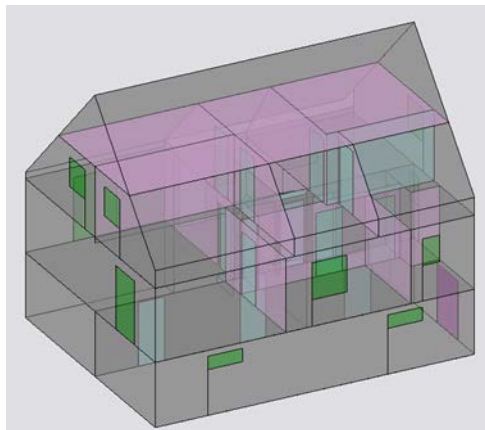


**Figure 2.34.** *Example of a representation of a residential environment*

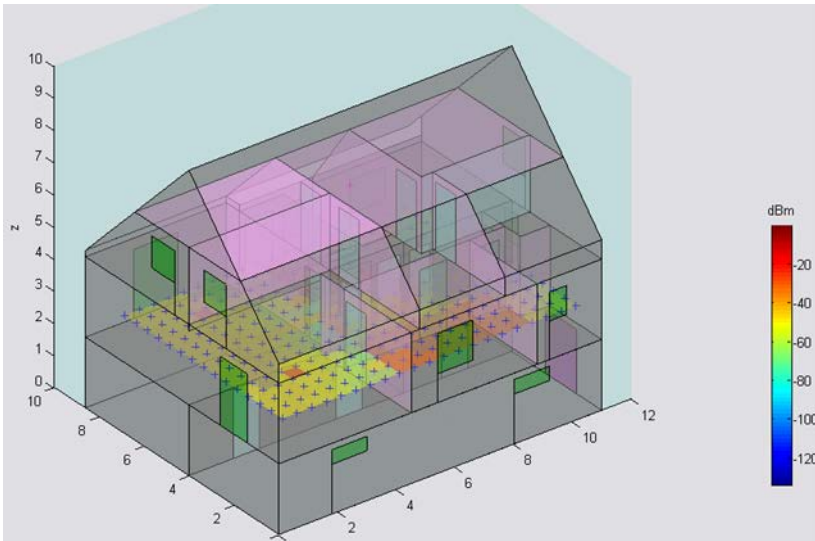


**Figure 2.35.** Example of radioelectric coverage in a residential environment

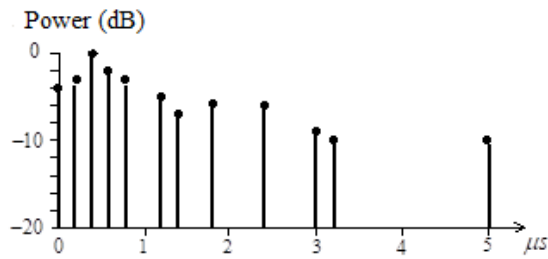


**Figure 2.36.** Schematic representation of a GSM TU channel with 12 paths

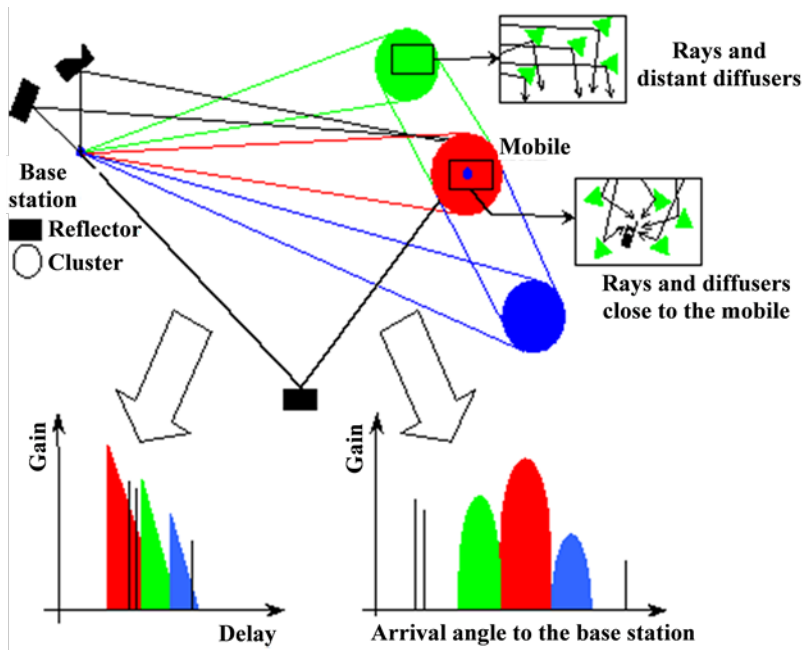


**Figure 2.37.** Relations between the position of reflectors and diffusers in the propagation environment; shape of the power time profile

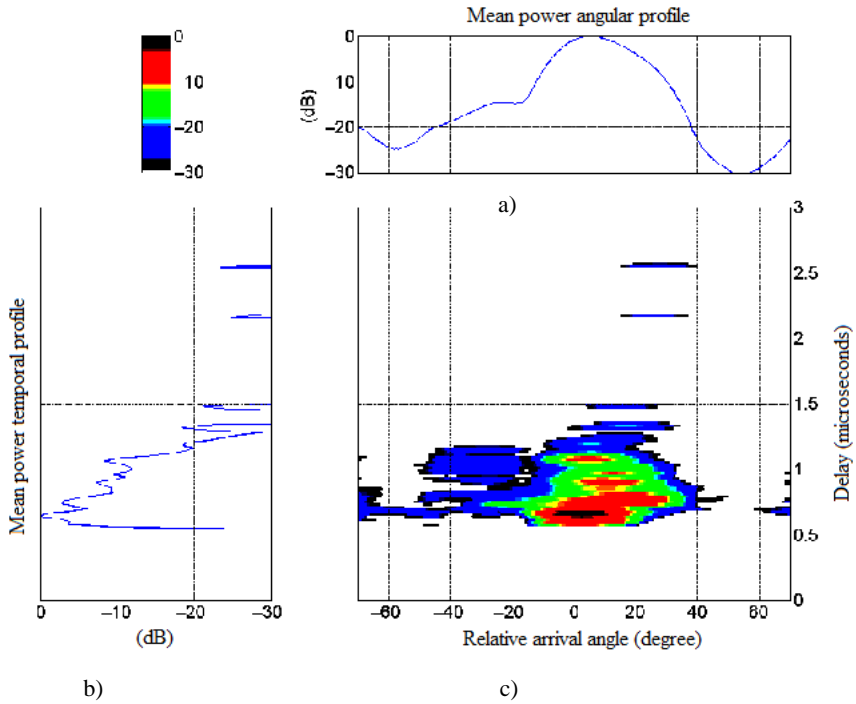


**Figure 2.38.** Spatiotemporal representation of the impulse response: a) angular power profile, b) temporal power profile, c) mean spatio-temporal power distribution, the origin of the angles corresponds to the pointing axis of the antenna at the base station

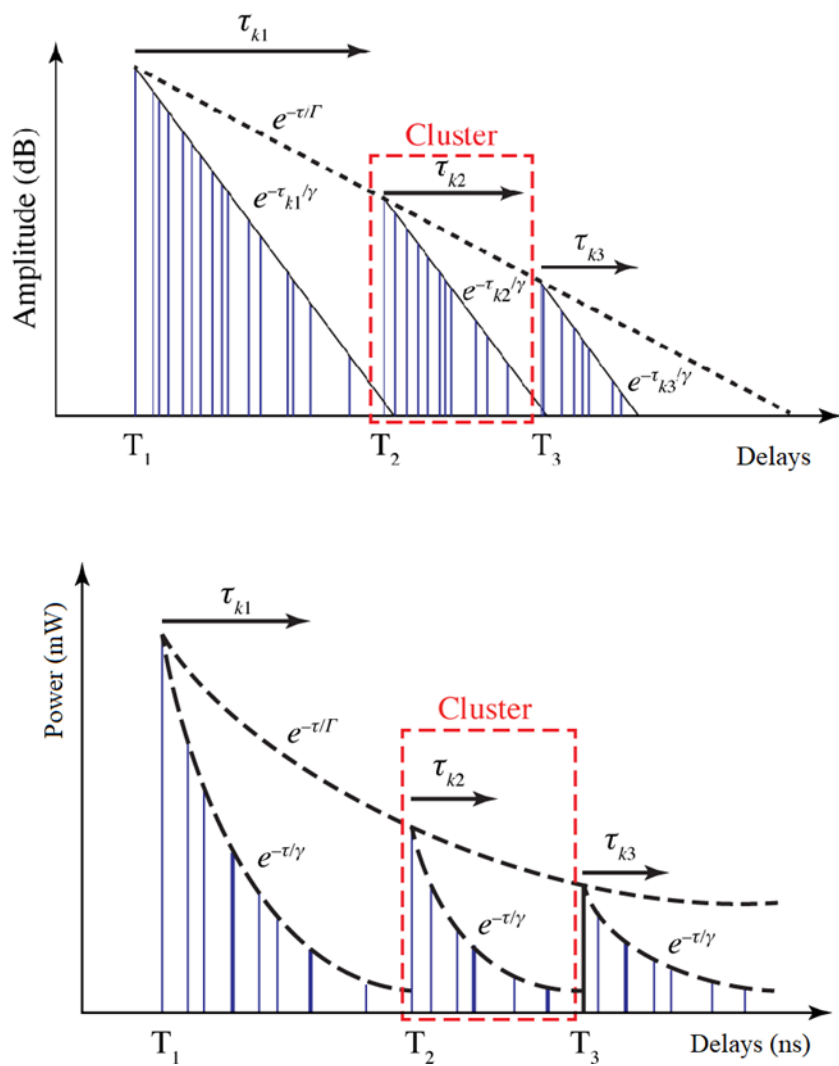


**Figure 2.39.** Power profile according to Saleh and Valenzuela formalism

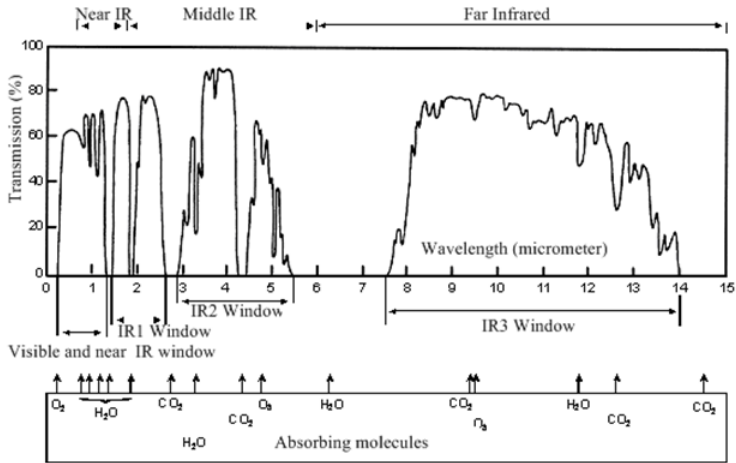


Figure 2.40. Transmittance of the atmosphere due to molecular absorption

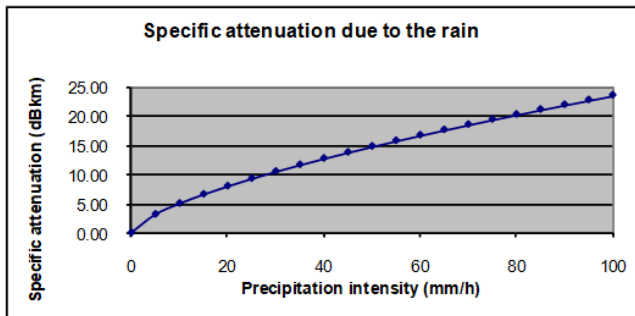


Figure 2.41. Specific attenuation (dB/km) due to rain in the optical and infrared range

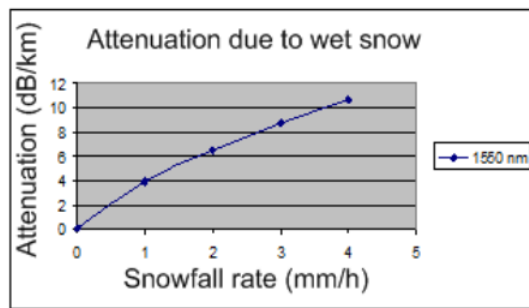
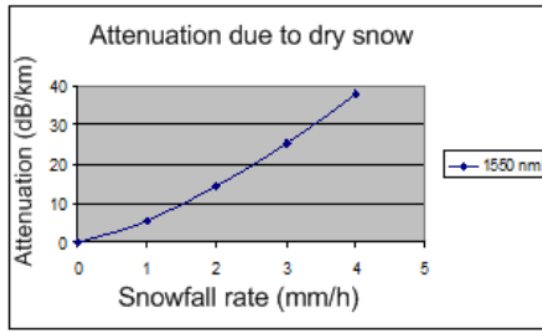
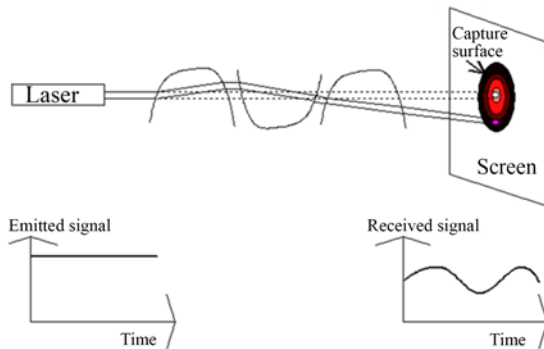


Figure 2.42. Wet snow: attenuation as a function of precipitation rate at 1,550 nm



**Figure 2.43.** Dry snow: attenuation as a function of precipitation rate at 1,550 nm



**Figure 2.44.** Deviation of the laser beam under the influence of turbulence cells greater than the beam diameter (deviation of the beam)

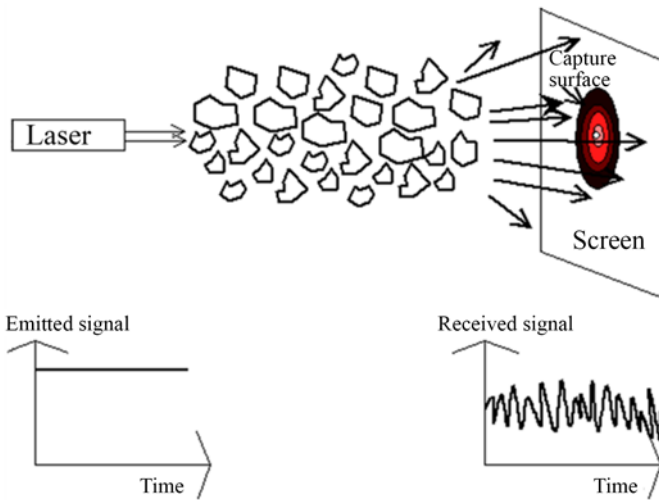


**Figure 2.45.** Deviation of the laser beam under the influence of turbulence cells smaller than the beam diameter (beam enlargement)

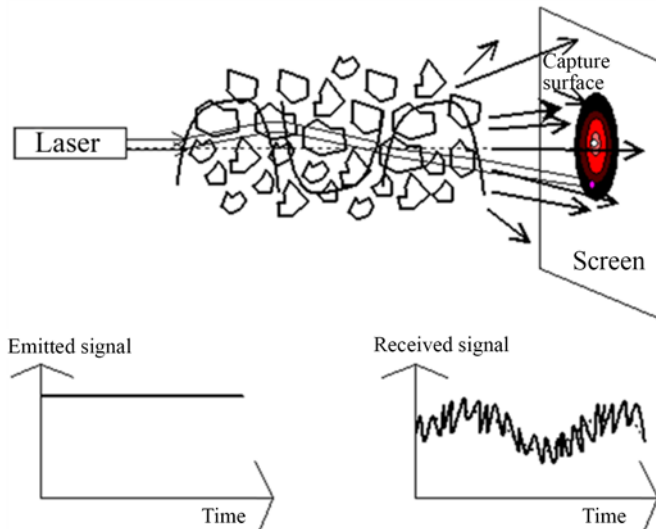


**Figure 2.46.** Effects of different heterogeneities and different sizes on the propagation of a laser beam (scintillations)

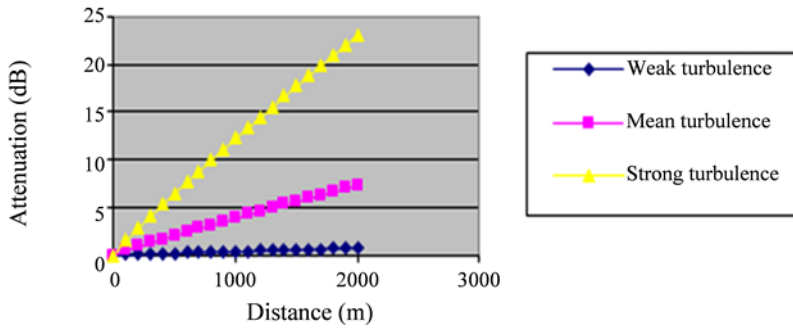


**Figure 2.47.** Variation in attenuation linked to the scintillation as a function of distance for different types of turbulence at 1.55 micron

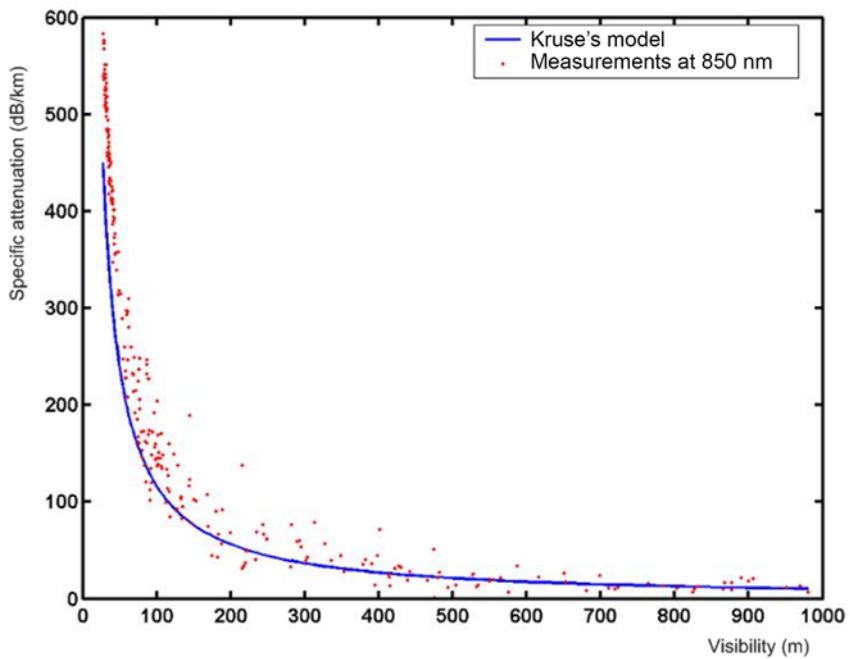


**Figure 2.48a.** Variation in specific attenuation at 850 nm as a function of visibility (comparison with the Kruse's model)

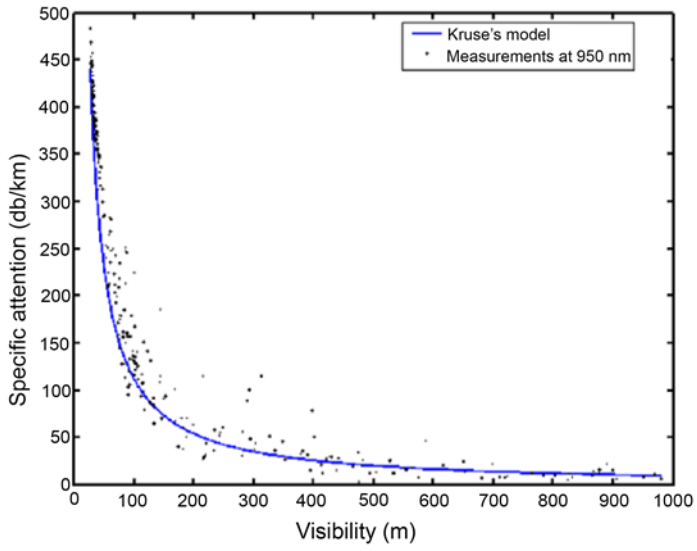


**Figure 2.48b.** Variation in specific attenuation at 950 nm as a function of visibility (comparison with the Kruse's model)

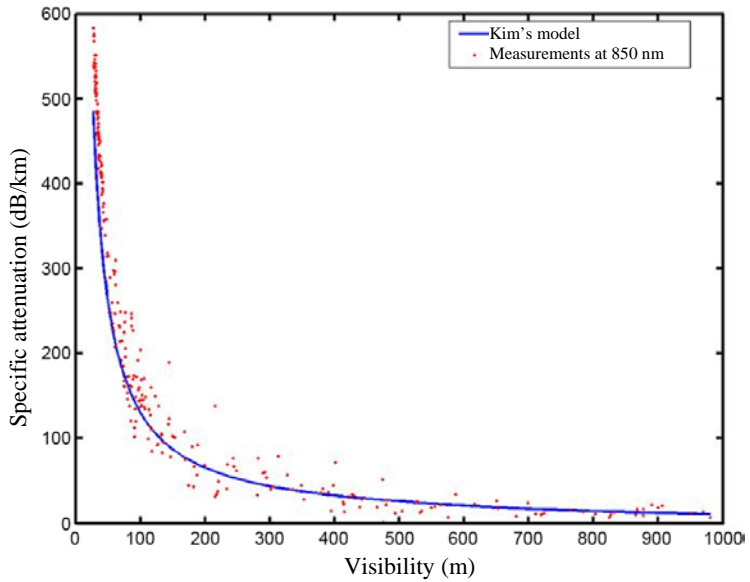


**Figure 2.49a.** Variation in specific attenuation at 850 nm as a function of visibility (comparison with Kim's model)

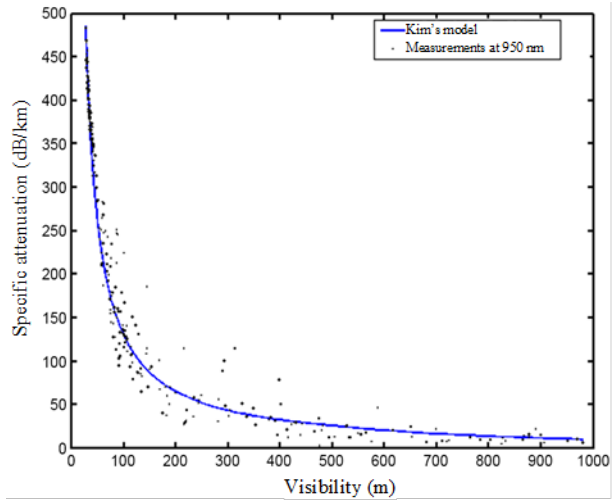


**Figure 2.49b.** Variation in specific attenuation at 950 nm as a function of visibility (comparison with Kim's model)

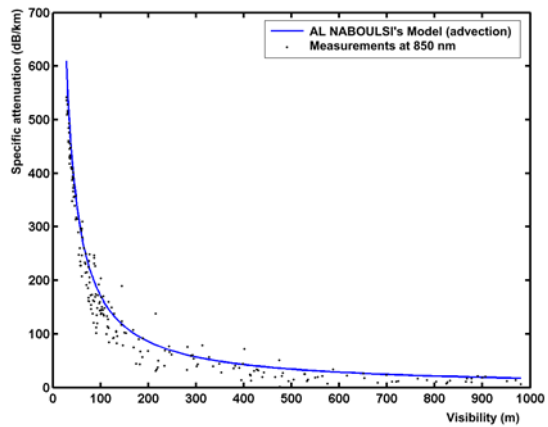


**Figure 2.50.** Variation in specific attenuation at 850 nm as a function of visibility (comparison with the Al Naboulsi advection model)

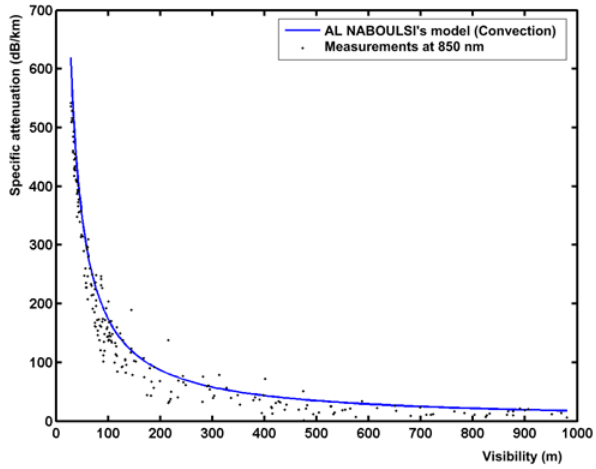


**Figure 2.51.** Variation in specific attenuation at 850 nm as a function of visibility (comparison with the Al Naboulsi convection model)

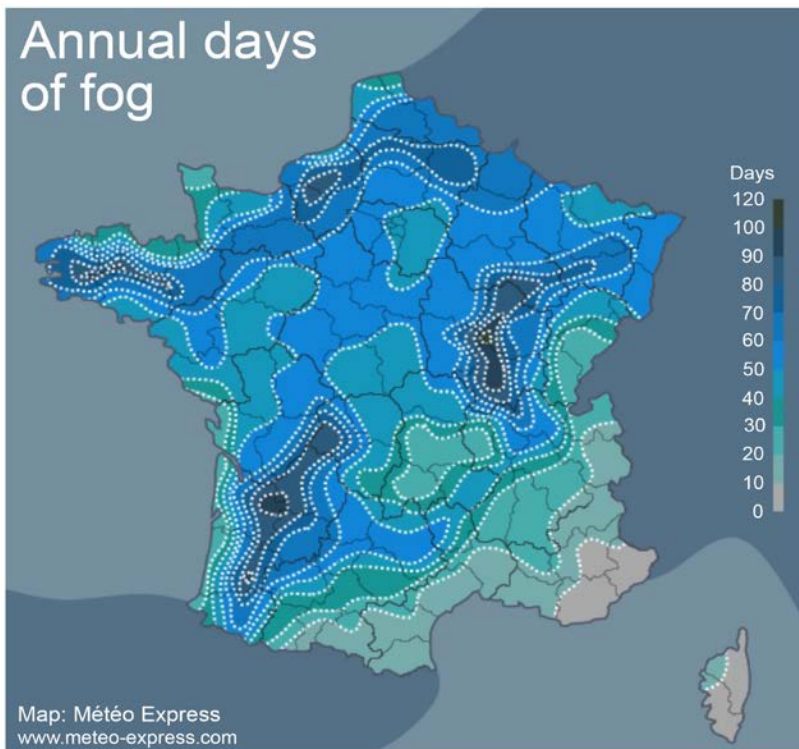


**Figure 2.52.** Number of days a year in France with fog (visibility less than 1 km)



**Figure 2.53.** Sandstorm (source: Wikipedia)

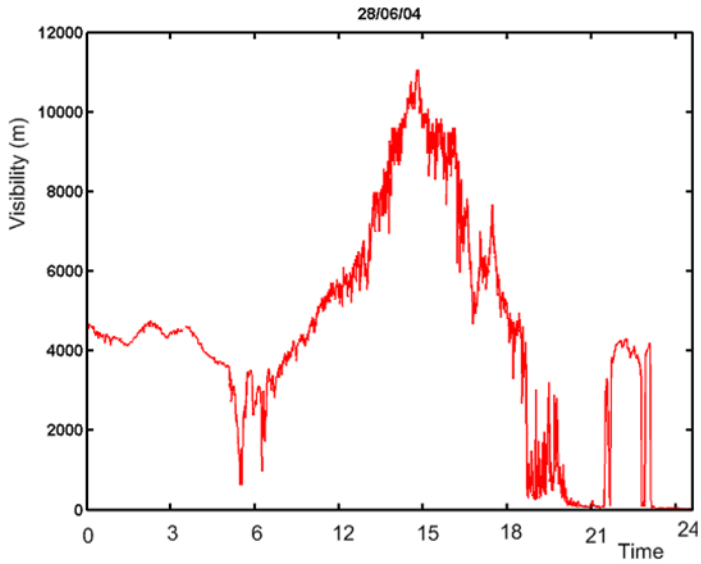


**Figure 2.54.** Variations in the MOR observed at the Turbie site on June 28, 2004

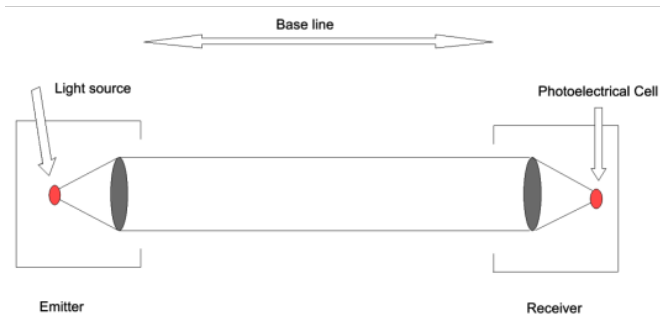


**Figure 2.55.** *Direct beam transmissometer*

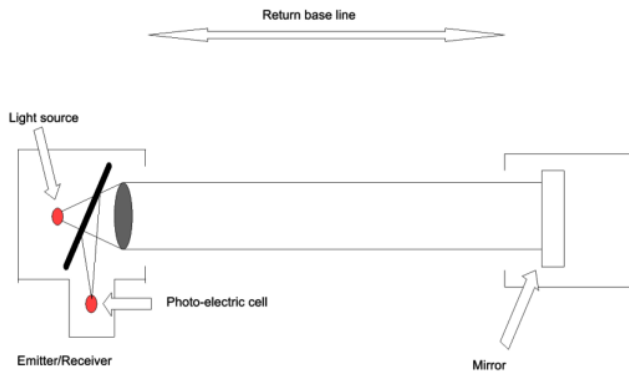


**Figure 2.56.** *Reflected beam transmissometer*

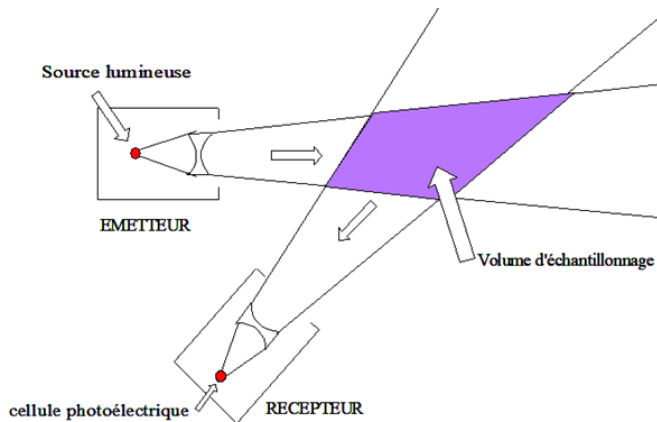


**Figure 2.57.** *Diagram showing the measurement of visibility by backscatter*

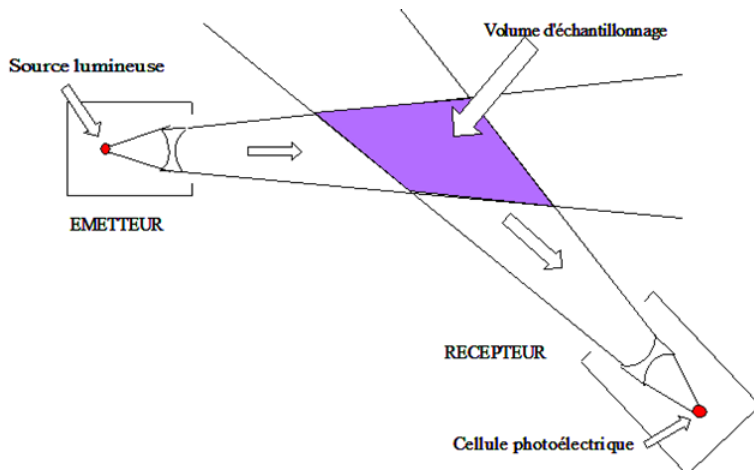


**Figure 2.58.** Diagram showing the measurement of visibility by forward scatter



